



Implementation of Intelligent Pneumonia Detection Model, Using Convolutional Neural Network (CNN) and InceptionV4 Transfer Learning Fine Tuning

Anggit Wirasto¹, Purwono², Muhammad Baballe Ahmad³

^{1,2} Universitas Harapan Bangsa, Purwokerto, Indonesia

³ Nigerian Defence Academy, Kaduna, Nigeria

ARTICLE INFO

Article history:

Received December 27, 2023

Revised February 28, 2024

Published March 01, 2024

Keywords:

Pneumonia;
CNN;
InceptionV4;
Transfer;
Learning;

ABSTRACT

In Pneumonia is a type of contagious lung infection that has caused many human deaths in the form of inflammation of the alveoli. Based on WHO data, pneumonia is a type of acute infection that has caused more than 450 million cases and 4 million deaths each year. Covid-19 is one of the global pandemics that triggered many pneumonia incidents. Chest X-rays (CXR) are an important part of patient care. Radiologists can use CXR features to determine the type of pneumonia and the underlying pathogenesis. Machine learning and deep learning technologies are used to automatically detect various human diseases, thus ensuring smart healthcare. CXR features are more suitable to be analyzed by convolutional neural network (CNN). This algorithm is one of the typical deep learning architectures that has strong characteristics that are widely applied in the healthcare field. This study aims to develop a deep learning-based paradigm to distinguish Covid-19 patients from healthy and normal individuals by analyzing the presence of pneumonia disease symptoms on the CXR. This research provides an approach to the use of InceptionV4 transfer learning type in performing classification on CXR images. There are three main approaches carried out, namely making a standard CNN model, optimizing transfer learning xception and fine tuning. The performance metrics results show a recall value close to 100% with a model accuracy value of 88%. Achieving a high enough recall value with a relatively small dataset makes the model built is considered to have good capabilities. The ability is also confirmed by the high ROC-AUC value with a value of 0.965.

This work is licensed under a [Creative Commons Attribution-Share Alike 4.0](https://creativecommons.org/licenses/by-sa/4.0/)



Corresponding Author:

Anggit Wirasto, Universitas Harapan Bangsa, Indonesia

Email: anggitwirasto@uhb.ac.id

1. INTRODUCTION

Various types of dangerous diseases continue to threaten people in the world. One of the diseases that is considered to be the most important health problem and a leading cause of death is Pneumonia[1]. This disease is a type of contagious lung infection that has caused many human deaths in the form of inflammation of the alveoli. This disease is a type of contagious lung infection that has caused many human deaths in the form of inflammation of the alveoli [2]. Based on WHO data, pneumonia is a type of acute infection that has caused more than 450 million cases and 4 million deaths each year [3].

Patients who have been diagnosed with pneumonia are usually treated empirically with antibiotics [4]. Pneumonia is divided into subcategories such as community-acquired, hospital-acquired, and ventilator-associated diseases, with each subcategory carrying different risk factors, morbidity and mortality, and possible pathogens, which require various antimicrobial regimens [4]. The condition of patients with pneumonia will also be worsened if the patient previously had heart failure. Patients admitted with pneumonia and heart failure have increased mortality and costs compared to patients without heart failure [5].

Covid-19 is one of the global pandemics[6]. which triggers a large incidence of pneumonia[7]. The lungs are the most affected organ of the human body by this pandemic. This not only affects respiratory problems, but also other organs such as the kidneys and liver [8]. The most common complication of coronavirus disease 2019 (COVID-19) associated pneumonia is acute respiratory distress syndrome (ARDS), which is characterized by dramatic inflammatory features such as cytokine release syndrome and macrophage activation syndrome (MAS)[9].

Chest X-rays (CXR) are an important part of patient care. Radiologists can use CXR features to determine the type of pneumonia and the underlying pathogenesis[10]. CXR is one of the most common radiologic examination methods for screening and diagnosis of chest diseases, as well as the main means of classifying and screening pneumonia, tuberculosis, and breast cancer, and is a painless and non-invasive examination method suitable for high populations at relatively low cost[11].

Machine learning and deep learning technologies are used to automatically detect various human diseases, thus ensuring smart healthcare[12]. Combination of deep learning algorithms and medical knowledge can improve medical staff performance[13]. And can also reduce patient waiting time by speeding up the diagnostic process and reducing the doctor's workload.

CXR features are more suitable for analysis with convolutional neural network (CNN)[13]. CNNs are useful for medical image classification so that they can help professionals and researchers develop new systems, provide more precise diagnosis, and start treatment as soon as possible[14]. CNN is one of the typical deep learning architectures that has strong characteristics that are widely applied in the healthcare field. CNN techniques can assist in the accurate detection and classification of COVID-19 along with the application of radiological imaging[15].

This study aims to develop a deep learning-based paradigm to distinguish Covid-19 patients from healthy and normal individuals by analyzing the presence of pneumonia disease symptoms on CXR. We intend to provide an approach to using InceptionV4 transfer learning type in performing classification on CXR images. The classification results will be used as a new deep learning model that will be analyzed for performance. Our contribution to this research can be summarized as follows:

- Collect and pre-process x-ray data.
- Building a CNN-based architecture to recognize x-rays of Covid-19 patients with InceptionV4 Transfer Learning.
- Performing fine tuning on the model that has been made
- Performing model evaluation

2. LITERATURE REVIEW

Many studies have explored various deep learning approaches to identify Covid-19 using clinical data such as CT scans and x-rays. For example, research that has been conducted by[16], which classified CXR images into COVID-19, Pneumonia and Tuberculosis using deep learning and XAI. The study used a single XAI-based CNN model to detect COVID-19, Pneumonia, and Tuberculosis diseases resulting in training accuracy of $95.76 \pm 1.15\%$, test accuracy of $94.31 \pm 1.01\%$, and validation accuracy of $94.54 \pm 1.33\%$

Research that has been conducted by [17] to improve the classification of COVID-19 CT CNNs by learning parameter-efficient representations. This research proposes the SR technique derived from contrastive learning and applies it to seven commonly used CNNs. Experimental results show that SR can stably improve CNN classification performance.

Research conducted by[18] utilizes an efficient ensemble for image-based pneumonia identification using deep CNN and SGD with warm restart. The experimental results show a significant improvement of SGDRE over the two baseline methods compared. With an achieved testing accuracy of 96.26% and AUC of 95.15%, the proposed method proved to be a highly competitive classification method.

Research conducted by[19] identified the Covid-19 infection status from chest x-ray images using a CNN-based architecture. The model can effectively distinguish other people from Covid-19 patients using x-rays. The suggested framework achieved 98.5% accuracy, 98.9% specificity, 99.0% sensitivity, 99.2%

precision, and 98.3% F1 score for three-class classification results. Research conducted by [20] conducted the application of PET/CT images under the convolutional neural network model in postoperative pneumonia virus infection monitoring of patients with small cell lung cancer. The results of this study found that the accuracy, sensitivity, and specificity of monitoring postoperative pneumonia virus infection in NSCLC patients through CNN model-based PET-CT images were high.

3. METHODS

3.1. Dataset

The dataset used in this study is secondary data taken from the kaggle site created by Tolga and can be accessed on the page <https://www.kaggle.com/datasets/tolgadincer/labeled-chest-xray-images>. The dataset contains 5,232 validated Chest X-ray images with the data structure as shown in Figure 2. The images are divided into a training set and an independent patient testing set. The dataset is divided into two main classes namely 'Pneumonia' and 'Normal'. The pneumonia class amounted to 3883 data, while the normal class amounted to 1349 data. In practice we need important features to optimize the performance of the data analysis task [21]. Available datasets can be polluted by other error-producing factors such as data inconsistencies and incomplete data. A data preprocessing stage is required to address these issues [22].



Fig. 1. (a) Normal, (b) Pneumonia

3.2. Preprocessing

Data processing is an important step before data is actually applied to machine learning [23]. This step is used to ensure the data is of good quality when used to train the model [22]. The image data generator technique was used in processing the chest x rays dataset. This technique was used to overcome the small dataset size and generate ten thousand additional images [23]. The input images are processed by converting them into floating-point tensors into the CNN. The stages used in this processing are (1) reading the image file stored in the folder, (2) decoding the JPEG content into RGB pixel grids with channels, (3) converting to floating-point tensors as input data to the CNN, (4) scaling the pixel values (between 0 and 255) to intervals between 0 and 1 [0,1].

The chest x rays dataset used appears to have imbalanced classes and in the medical world this is a common problem in deep learning-based classifiers [24] [25]. Class imbalance occurs when some classes have significantly more samples in the training dataset than others. It has been shown that class imbalance can negatively impact the training of CNN models [29]. The solution to this can be done by using oversampling techniques that have been widely used in deep learning and have proven to be reliable. The SMOTE oversampling technique is a more advanced oversampling technique that attempts to solve this problem. It generates new synthetic samples by interpolating the closest data [26]. In this study, 80% of the preprocessing data was used for training, while 20% was used for model testing and validation.

3.3. CNN Model

CNN have a good capacity in learning image representations [27]. CNN is a model that can generate feature maps sequentially, acquiring simple characteristics of data such as vertices and edges of images at the first layer and clustering them into more complex patterns [28]. These feature maps are obtained by applying a convolutional operation with a trainable kernel to the input layer [28]. Non-linear transformation and pooling are complementary functions that help the network to converge [28]. A prediction is then generated based on

the processed feature maps [28]. The CNN architecture consists of a total of 5 weight layers with 3 convolutional layers each followed by a ReLU activation function and max-pooling operation, and 2 fully-connected layers with a final softmax classifier[29].

3.4. InceptionV4 Transfer Learning

In this study we performed InceptionV4 implementations that were trained with 50 epochs each. The model is built with a loss function of binary cross entropy with Adam optimizers. The InceptionV4 network replaces the convolution in the inception v3 architecture with deep separable convolution, thus increasing the width of the network and reducing the number of parameters and calculations of the model[30]. At the same time, a residual connection mechanism similar to the ResNet network is introduced to accelerate the convergence of the network, improve the classification accuracy value to increase the learning ability of the network to more detailed features. [31]. This model includes an input layer, convolution layer, fully connected layer and output layer. In this model, there is a deeply separable convolution layer in the convolution layer, which is linearly connected to the residual. The InceptionV4 network model contains 36 convolution layers and consists of 14 modules. In addition to the first module and the last module, other models adopt the linear connection operation in the general network model and the residual connection of structure [31]. According to the schematic diagram of the InceptionV4 model[31], It can be found that depth separable convolution is not directly used in the model. The positions of the convolution kernels of 3 x 3 and 1 x 1 are interchanged sequentially.

The pre-processed images are passed to the InceptionV4 model. It is a type of 71-layer 2 CNN inspired by google's Inception model and based on a radical interpretation of the Inception model[32]. This stage employs depth-separable convolutional layers[18]. The process starts with 1x1 point-wise convolution and then moves to 3x3 depth wise convolution followed by logistic regression. The standard architecture of the InceptionV4 model can be seen in Figure 3.[33].

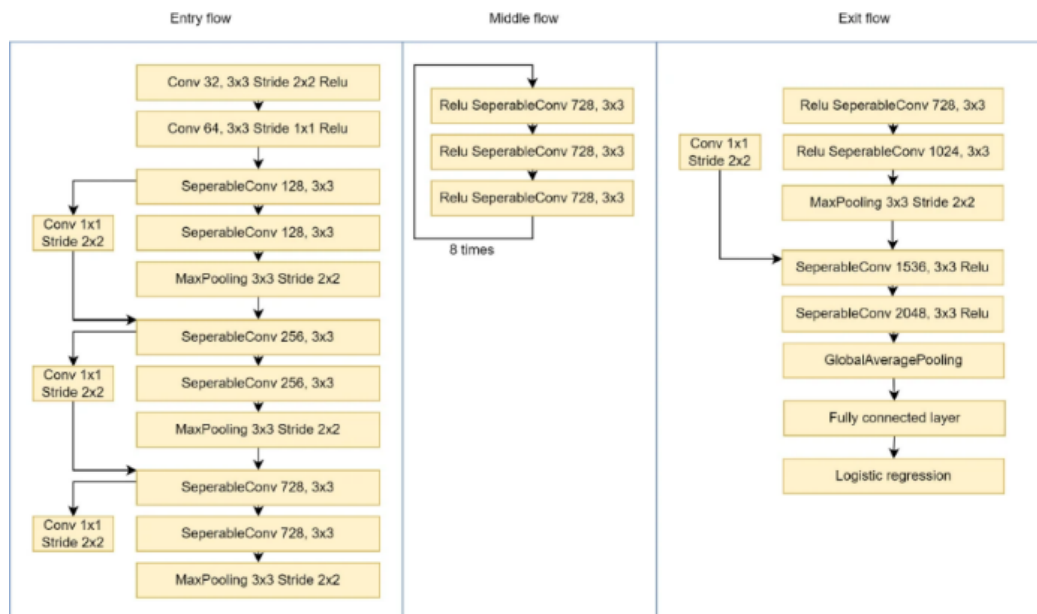


Fig. 2. Standard InceptionV4 architecture

3.5. Fine Tuning

Fine tuning has built great interest for researchers due to its relevance for retraining convolutional networks for many and interesting applications[34]. For object classification, detection, and segmentation, the model enhanced with this technique has shown better results. In the last section, all layers of the pre-training model are frozen to retain the weights calculated during its training on the ImageNet dataset. In the next step, it unfreezes its last few layers and continues training, adjusting the weights of these layers according to our data set.

3.6. Performance Metrics

The evaluation of the metrics used in this CNN classification uses the standard method, namely the confusion matrix. The model evaluation used is accuracy, precision, recall, f1-score and the area of the receiver operating characteristic (ROC) curve and the area under a ROC Curve (AUC)[41]. Accuracy is the capacity of the system to correctly determine the type of AD. The formula used to calculate accuracy is as follows.

$$Accuracy = \frac{TP + TN}{TP + TN + FP + FN} \quad (1)$$

Specificity is the capacity of the system to correctly identify true alzheimer's using the following formula.

$$Specificity = \frac{TN}{TP + TN} \quad (2)$$

Sensitivity is the capacity of the model to correctly classify alzheimer's with the following formula.

$$Sensitivity = \frac{TP}{TP + FN} \quad (3)$$

Precision is the closeness of two measured values to each other with the following formula.

$$Precision = \frac{TP}{TP + FP} \quad (4)$$

F1-Score is the harmonic mean of precision and recall. The formula used is as follows.

$$F1 - Score = 2x \frac{(Recall * Precision)}{(Recall + Precision)} \quad (5)$$

where, the parameters are TP = true positive, TN = true negative, FP = false positive, and FN = false negative.

The area under the receiver operating characteristic (ROC) curve, or AUC for short, is a single scalar value that measures the overall performance of a binary classifier. AUC values are in the range [0.5-1.0], where the minimum value represents the performance of a random classifier and the maximum value would correspond to a perfect classifier[42].

4. RESULTS AND DISCUSSION

4.1. Experimental Setup

In this paper, the experiments used 64-bit Windows 10 operating system to implement the algorithm. The processor used is 11th Gen Intel(R) Core(TM) i7-1165G7 @ 2.80GHz 2.80 GHz with 16 GB RAM capacity. Python programming language was implemented in Jupyter Notebook application using GPU 100 accelerator. Pre-training was conducted on ImageNet dataset.CNN Model

The image data processing stage produces what has been done followed by making a CNN model. At this stage we configure the parameters that will be used by the model. Parameters are weights that are learned during training. They are weight matrices that contribute to the predictive power of the model, and change during the back propagation process. The CNN model that was built can be seen in Table 1..

Table 1. Table Styles

Layer (type)	Output Shape	Param
input_1 (InputLayer)	[(None, 224, 224, 3)]	0
conv2d (Conv2D)	(None, 222, 222, 16)	448
batch_normalization (BatchNo	(None, 222, 222, 16)	64
activation (Activation)	(None, 222, 222, 16)	0
max_pooling2d (MaxPooling2D)	(None, 111, 111, 16)	0
dropout (Dropout)	(None, 111, 111, 16)	0

conv2d_1 (Conv2D)	(None, 109, 109, 32)	4640
batch_normalization_1	(None, 109, 109, 32)	128
activation_1 (Activation)	(None, 109, 109, 32)	0
max_pooling2d_1 (MaxPooling2)	(None, 54, 54, 32)	0
dropout_1 (Dropout)	(None, 54, 54, 32)	0
conv2d_2 (Conv2D)	(None, 52, 52, 64)	18496
conv2d_3 (Conv2D)	(None, 50, 50, 64)	36928
batch_normalization_2 (Batch)	(None, 50, 50, 64)	256
activation_2 (Activation)	(None, 50, 50, 64)	0
max_pooling2d_2 (MaxPooling2)	(None, 25, 25, 64)	0
dropout_2 (Dropout)	(None, 25, 25, 64)	0
flatten (Flatten)	(None, 40000)	0
dense (Dense)	(None, 64)	2560064
dropout_3 (Dropout)	(None, 64)	0
dense_1 (Dense)	(None, 1)	65

The CNN model that has been formed is then subjected to a fitting process to measure how well the machine learning model is able to generalize data similar to the one it was trained on. A well-fitted model produces more accurate results. At this stage, 50 epochs are run. The results of this fitting process are model evaluation in the form of learning curve loss validation which can be seen in Figure 4 and learning curve accuracy which can be seen in Figure 5. The validation loss value is 0.13492867350578308 and validation accuracy is 0.9522445201873779. The evaluation value of the testing model is a test loss with a score of 0.4296790361404419 and a test accuracy of 0.8493589758872986. The curve graph shows that the loss value is decreasing and the accuracy value tends to increase.

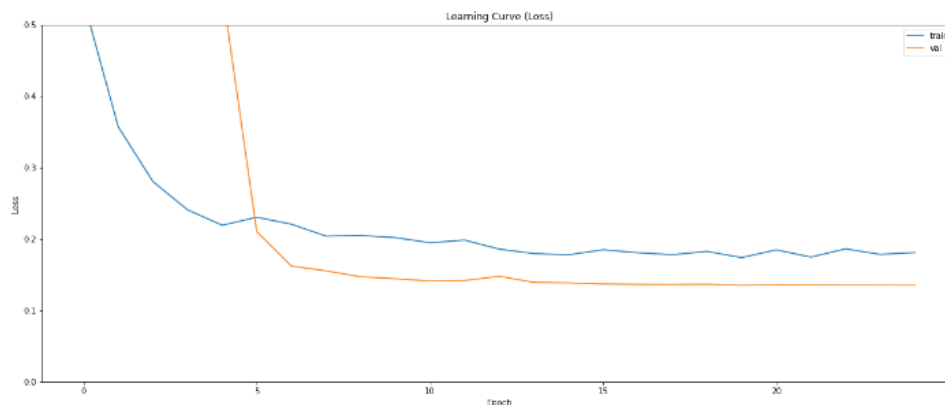


Fig. 3. Learning curve loss validation.

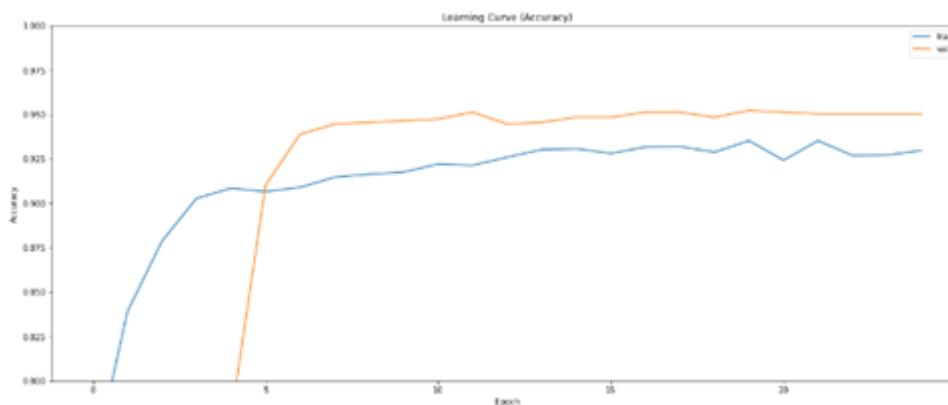


Fig. 4. Learning curve accuracy validation.

4.2. Transfer Learning

The second approach, called transfer learning, consists of using a pre-training model as a feature extractor. In this research, the model chosen was InceptionV4. This model was already trained on another dataset (ImageNet). The transfer learning process with InceptionV4 is done by setting `include_top = 'false'`, removing 'head', which is responsible for assigning classes in this other dataset, and keeping all previous layers. Then, the last few layers are also included, including the layer responsible for generating the output. The CNN model that has gone through the InceptionV4 transfer learning approach can be seen in Table 2.

Table 2. CNN InceptionV4 Transfer Learning

Layer (type)	Output Shape	Param
input_1 (InputLayer)	[(None, 224, 224, 3)]	0
InceptionV4 (Functional)	(None, None, None, 2048)	20861480
global_average_pooling2d	(None, 2048)	0
dense (Dense)	(None, 128)	262272
dropout (Dropout)	(None, 128)	0
dense_1 (Dense)	(None, 1)	129

The results of the transfer learning process with InceptionV4 are evaluated again in the form of learning curve loss validation which can be seen in Figure 6 and learning curve accuracy which can be seen in Figure 7. The validation loss value is 0.1567215770483017 and validation accuracy is 0.9493792057037354. The evaluation value of the testing model is a test loss with a score of 0.26238813996315 and a test accuracy of 0.9006410241127014. The curve graph shows that the loss value is decreasing and the accuracy value tends to increase.

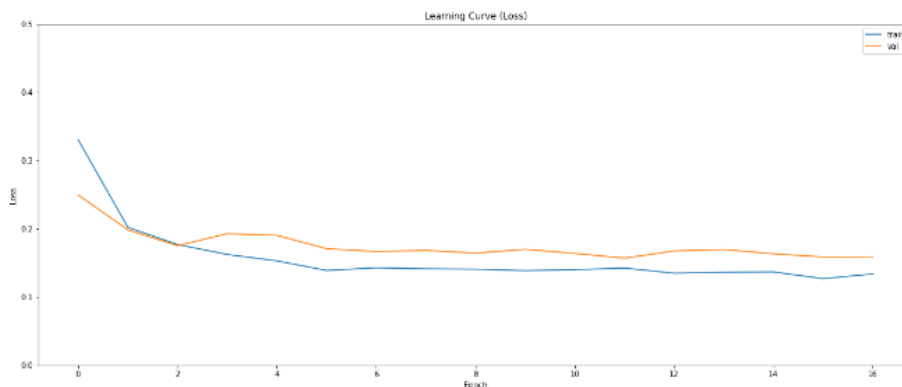


Fig. 6. InceptionV4 Learning Curve Accuracy Validation.

4.3. Performance Metrics

The confusion matrix method is used as an evaluation of the results of the CNN classification model in this study. Confusion matrix produces accuracy, recall, precision and f1-score values. The performance metrics graph for this testing data can be seen in Figure 10, while for the ROC curve can be seen in Figure 11. Table 4 is the result of the performance of the CNN model test data that has used InceptionV4 and fine tuning.

Table 4. Performance Matrix

Class	Precision	Recall	F1-Score
0	0.94	0.71	0.81
1	0.85	0.97	0.91
accuracy			0.88
macro avg	0.90	0.84	0.86
weighted avg	0.89	0.88	0.87

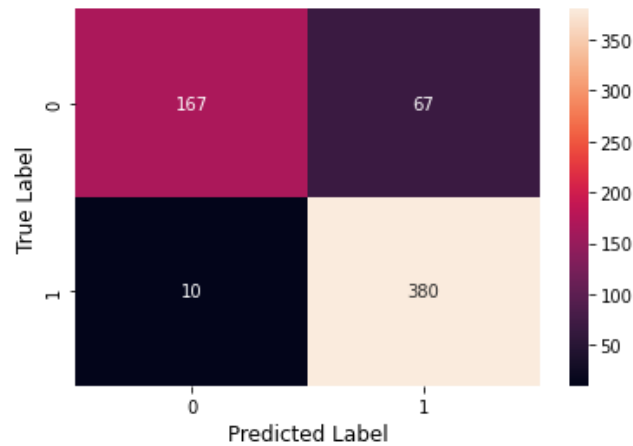


Fig. 8. Confusion Matrix

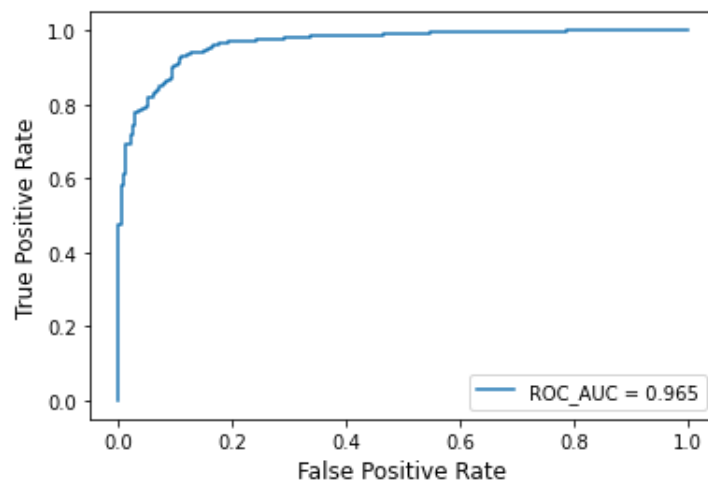


Fig. 9. ROC AUC.

Based on the results in Table 4, the recall value is close to 100%. Achieving a fairly high recall value with a relatively small set of datasets makes the model built is considered to have good capabilities. This ability is also confirmed by the high ROC-AUC value with a value of 0.965.

5. CONCLUSION

Based on the experimental results that have been conducted in this study, we conclude that there are several processes that have been carried out to produce a pneumonia classification model with CNN that has quite good capabilities. The process begins with the selection of the Chest X Rays dataset followed by the data processing stage. The next stage is the creation of a standard CNN model that is run with 50 epochs. The results of making the initial model in the form of a validation loss value of 0.13492867350578308 and validation accuracy of 0.9522445201873779. The evaluation value of the testing model is in the form of a test loss with a score of 0.4296790361404419 and a test accuracy of 0.8493589758872986. The curve graph shows that the loss value is decreasing and the accuracy value tends to increase. The second approach is to optimize the model with InceptionV4 transfer learning. The results of this transfer learning process produce a validation loss value of 0.1567215770483017 and validation accuracy of 0.9493792057037354. The evaluation value of the testing model is a test loss with a score of 0.26238813996315 and test accuracy of 0.9006410241127014. The curve graph shows that the loss value is decreasing and the accuracy value tends to increase. The last approach of making this CNN model is fine tuning. The results of this fine tuning process are carried out model evaluation again with a validation loss value of 0.1509828865281067 and validation accuracy of 0.9493792057037354. The evaluation value of the testing model is in the form of a test loss with a score of 0.2820434272289276 and test accuracy of 0.8766025900840759. The curve graph shows that the loss value is decreasing and the accuracy

value tends to increase. The performance metrics results show a recall value close to 100% with a model accuracy value of 88%. Achieving a fairly high recall value with a relatively small dataset makes the model built is considered to have good capabilities. This ability is also confirmed by the high ROC-AUC value with a value of 0.965.

REFERENCES

- [1] S. Kiliçarslan, C. Közkurt, S. Baş, and A. Elen, "Detection and classification of pneumonia using novel Superior Exponential (SupEx) activation function in convolutional neural networks," *Expert Syst Appl*, vol. 217, p. 119503, 2023, doi: <https://doi.org/10.1016/j.eswa.2023.119503>.
- [2] H. Liz, M. Sánchez-Montañés, A. Tagarro, S. Domínguez-Rodríguez, R. Dagan, and D. Camacho, "Ensembles of Convolutional Neural Network models for pediatric pneumonia diagnosis," *Future Generation Computer Systems*, vol. 122, pp. 220–233, 2021, doi: <https://doi.org/10.1016/j.future.2021.04.007>.
- [3] M. W. Kusk and S. Lysdahlgaard, "The effect of Gaussian noise on pneumonia detection on chest radiographs, using convolutional neural networks," *Radiography*, vol. 29, no. 1, pp. 38–43, 2023, doi: <https://doi.org/10.1016/j.radi.2022.09.011>.
- [4] S. J. Wolf *et al.*, "Clinical Policy: Critical Issues in the Management of Adult Patients Presenting to the Emergency Department With Community-Acquired Pneumonia," *Ann Emerg Med*, vol. 77, no. 1, pp. e1–e57, 2021, doi: <https://doi.org/10.1016/j.annemergmed.2020.10.024>.
- [5] J. El Halabi *et al.*, "Differential Impact of Systolic and Diastolic Heart Failure on In-Hospital Treatment, Outcomes, and Cost of Patients Admitted for Pneumonia," *American Journal of Medicine Open*, p. 100025, 2022, doi: <https://doi.org/10.1016/j.ajmo.2022.100025>.
- [6] R. D. Goldman *et al.*, "Willingness to vaccinate children against COVID-19 declined during the pandemic," *Vaccine*, 2023, doi: <https://doi.org/10.1016/j.vaccine.2023.02.069>.
- [7] N. Shaker, J. P. Rosenheck, B. A. Whitson, and K. Shilo, "Pulmonary hematoidin deposition in a case of severe COVID19 pneumonia," *Human Pathology Reports*, vol. 27, p. 300601, 2022, doi: <https://doi.org/10.1016/j.hpr.2022.300601>.
- [8] N. Sri Kavya, T. shilpa, N. Veeranjanyulu, and D. Divya Priya, "Detecting Covid19 and pneumonia from chest X-ray images using deep convolutional neural networks," *Mater Today Proc*, vol. 64, pp. 737–743, 2022, doi: <https://doi.org/10.1016/j.matpr.2022.05.199>.
- [9] S. Piconi, S. Pontiggia, M. Franzetti, F. Branda, and D. Tosi, "Statistical models to predict clinical outcomes with anakinra vs. tocilizumab treatments for severe pneumonia in COVID19 patients," *Eur J Intern Med*, 2023, doi: <https://doi.org/10.1016/j.ejim.2023.01.024>.
- [10] X. Ying, H. Liu, and R. Huang, "COVID-19 chest X-ray image classification in the presence of noisy labels," *Displays*, vol. 77, p. 102370, 2023, doi: <https://doi.org/10.1016/j.displa.2023.102370>.
- [11] L. Kong and J. Cheng, "Classification and detection of COVID-19 X-Ray images based on DenseNet and VGG16 feature fusion," *Biomed Signal Process Control*, vol. 77, p. 103772, 2022, doi: <https://doi.org/10.1016/j.bspc.2022.103772>.
- [12] H. Naeem and A. A. Bin-Salem, "A CNN-LSTM network with multi-level feature extraction-based approach for automated detection of coronavirus from CT scan and X-ray images," *Appl Soft Comput*, vol. 113, p. 107918, 2021, doi: <https://doi.org/10.1016/j.asoc.2021.107918>.
- [13] H. Liz, J. Huertas-Tato, M. Sánchez-Montañés, J. Del Ser, and D. Camacho, "Deep learning for understanding multilabel imbalanced Chest X-ray datasets," *Future Generation Computer Systems*, 2023, doi: <https://doi.org/10.1016/j.future.2023.03.005>.
- [14] L. F. de J. Silva, O. A. C. Cortes, and J. O. B. Diniz, "A novel ensemble CNN model for COVID-19 classification in computerized tomography scans," *Results in Control and Optimization*, vol. 11, p. 100215, 2023, doi: <https://doi.org/10.1016/j.rico.2023.100215>.
- [15] Md. B. Hossain, S. M. H. S. Iqbal, Md. M. Islam, Md. N. Akhtar, and I. H. Sarker, "Transfer learning with fine-tuned deep CNN ResNet50 model for classifying COVID-19 from chest X-ray images," *Inform Med Unlocked*, vol. 30, p. 100916, 2022, doi: <https://doi.org/10.1016/j.imu.2022.100916>.

- [16] M. Bhandari, T. B. Shahi, B. Siku, and A. Neupane, "Explanatory classification of CXR images into COVID-19, Pneumonia and Tuberculosis using deep learning and XAI," *Comput Biol Med*, vol. 150, p. 106156, 2022, doi: <https://doi.org/10.1016/j.compbiomed.2022.106156>.
- [17] Y. Xu, H.-K. Lam, G. Jia, J. Jiang, J. Liao, and X. Bao, "Improving COVID-19 CT classification of CNNs by learning parameter-efficient representation," *Comput Biol Med*, vol. 152, p. 106417, 2023, doi: <https://doi.org/10.1016/j.compbiomed.2022.106417>.
- [18] G. Vrbančić and V. Podgorelec, "Efficient ensemble for image-based identification of Pneumonia utilizing deep CNN and SGD with warm restarts," *Expert Syst Appl*, vol. 187, p. 115834, 2022, doi: <https://doi.org/10.1016/j.eswa.2021.115834>.
- [19] P. Ghose, Md. A. Uddin, U. K. Acharjee, and S. Sharmin, "Deep viewing for the identification of Covid-19 infection status from chest X-Ray image using CNN based architecture," *Intelligent Systems with Applications*, vol. 16, p. 200130, 2022, doi: <https://doi.org/10.1016/j.iswa.2022.200130>.
- [20] J. Wei, R. Zhu, H. Zhang, P. Li, A. Okasha, and A. K. H. Muttar, "Application of PET/CT image under convolutional neural network model in postoperative pneumonia virus infection monitoring of patients with non-small cell lung cancer," *Results Phys*, vol. 26, p. 104385, 2021, doi: <https://doi.org/10.1016/j.rinp.2021.104385>.
- [21] Z. Wang, L. Xia, H. Yuan, R. S. Srinivasan, and X. Song, "Principles, research status, and prospects of feature engineering for data-driven building energy prediction: A comprehensive review," *Journal of Building Engineering*, vol. 58, p. 105028, 2022, doi: <https://doi.org/10.1016/j.jobe.2022.105028>.
- [22] R. Nyirandayisabye, H. Li, Q. Dong, T. Hakuzweyezu, and F. Nkinahamira, "Automatic pavement damage predictions using various machine learning algorithms: Evaluation and comparison," *Results in Engineering*, vol. 16, p. 100657, 2022, doi: <https://doi.org/10.1016/j.rineng.2022.100657>.
- [23] I. S. Mangkunegara and P. Purwono, "Analysis of DNA Sequence Classification Using SVM Model with Hyperparameter Tuning Grid Search CV," in *2022 IEEE International Conference on Cybernetics and Computational Intelligence (CyberneticsCom)*, 2022, pp. 427–432. doi: [10.1109/CyberneticsCom55287.2022.9865624](https://doi.org/10.1109/CyberneticsCom55287.2022.9865624).
- [24] E. Tartaglione, C. A. Barbano, C. Berzovini, M. Calandri, and M. Grangetto, "Unveiling COVID-19 from CHEST X-Ray with Deep Learning: A Hurdles Race with Small Data.," *Int J Environ Res Public Health*, vol. 17, no. 18, Sep. 2020, doi: [10.3390/ijerph17186933](https://doi.org/10.3390/ijerph17186933).
- [25] M. M. Islam, F. Karray, R. Alhajj, and J. Zeng, "A Review on Deep Learning Techniques for the Diagnosis of Novel Coronavirus (COVID-19)," *IEEE Access*, vol. 9, pp. 30551–30572, 2021, doi: [10.1109/ACCESS.2021.3058537](https://doi.org/10.1109/ACCESS.2021.3058537).
- [26] E. Chamseddine, N. Mansouri, M. Soui, and M. Abed, "Handling class imbalance in COVID-19 chest X-ray images classification: Using SMOTE and weighted loss," *Appl Soft Comput*, vol. 129, p. 109588, 2022, doi: <https://doi.org/10.1016/j.asoc.2022.109588>.
- [27] S. S. Dambal, M. K. Doddananjedevuru, and S. B. Gopalakrishna, "Premature Ventricular Contraction Classification Based on Spiral Search - Manta Ray Foraging and Bi-LSTM," *International Journal of Intelligent Engineering and Systems*, vol. 15, no. 6, pp. 1–10, 2022, doi: [10.22266/ijies2022.1231.01](https://doi.org/10.22266/ijies2022.1231.01).
- [28] S. Bringas, S. Salomón, R. Duque, C. Lage, and J. L. Montaña, "Alzheimer's Disease stage identification using deep learning models," *J Biomed Inform*, vol. 109, p. 103514, 2020, doi: <https://doi.org/10.1016/j.jbi.2020.103514>.
- [29] L. Falaschetti, L. Manoni, D. Di Leo, D. Pau, V. Tomaselli, and C. Turchetti, "A CNN-based image detector for plant leaf diseases classification," *HardwareX*, vol. 12, p. e00363, 2022, doi: <https://doi.org/10.1016/j.ohx.2022.e00363>.
- [30] H. Chen, Y. Yang, and S. Zhang, "Learning Robust Scene Classification Model with Data Augmentation Based on Xception," *J Phys Conf Ser*, vol. 1575, no. 1, p. 12009, 2020, doi: [10.1088/1742-6596/1575/1/012009](https://doi.org/10.1088/1742-6596/1575/1/012009).
- [31] Y. Zhu, H. JiaYI, Y. Li, and W. Li, "Image identification of cashmere and wool fibers based on the improved Xception network," *Journal of King Saud University - Computer and Information Sciences*, 2022, doi: <https://doi.org/10.1016/j.jksuci.2022.09.009>.
- [32] C. Upasana, A. S. Tewari, and J. P. Singh, "An Attention-based Pneumothorax Classification using Modified Xception Model," *Procedia Comput Sci*, vol. 218, pp. 74–82, 2023, doi: <https://doi.org/10.1016/j.procs.2022.12.403>.
- [33] B. Gülmez, "A novel deep neural network model based Xception and genetic algorithm for detection of COVID-19 from X-ray images," *Ann Oper Res*, 2022, doi: [10.1007/s10479-022-05151-y](https://doi.org/10.1007/s10479-022-05151-y).

-
- [34] C. Amisse, M. E. Jijón-Palma, and J. A. Silva Centeno, "Fine-tuning deep learning models for pedestrian detection," *Boletim de Ciencias Geodesicas*, vol. 27, no. 2, pp. 1–16, 2021, doi: 10.1590/S1982-21702021000200013.